Research Network FWF S105

Photoacoustic Imaging in Medicine and Biology

http://www.csc.univie.ac.at/pai/

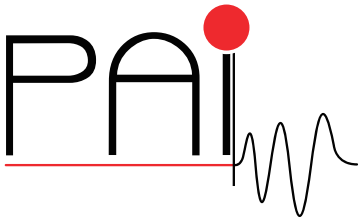

Photoacoustic Tomography with integrating fiber-based annular detectors

Hubert Grün, Halit Altmisdört, Thomas Berer, Günther Paltauf, Gerhard Zangerl, Markus Haltmeier and Peter Burgholzer

February 2011

PAI Report No. 34

FWF

Der Wissenschaftsfonds.

Photoacoustic tomography with integrating fiber-based annular detectors

H. Grün[a], H. Altmisdört[a], T. Berer[a], G. Paltauf[b], G. Zangerl[c], M. Haltmeier[c] and P. Burgholzer[a]

[a]RECENDT Research Center for Non Destructive Testing GmbH, Linz, Austria;
[b]Karl-Franzens-University, Dep. of Physics, Graz, Austria
[c]University of Vienna, Computational Science Center, Wien, Austria

ABSTRACT

Photoacoustic tomography is an emerging technology combining the advantages of optical imaging (high contrast) and ultrasonic imaging (high spatial resolution). Applications for photoacoustic tomography are mainly in imaging soft tissue. For photoacoustic imaging the sample is illuminated by a short pulse of electromagnetic energy. Depending on the specific absorption rate (SAR) the electromagnetic radiation is absorbed and the subsequent thermoelastic expansion launches broadband ultrasonic waves. Usually point like piezo-electric detectors are used. Our group introduced integrating detectors a few years ago. This type of detector integrates the pressure at least along one dimension. Integrating line detectors, which integrate the pressure along one dimension, can be realized by using either free-beam or fiber-based interferometers. The latter approach also allows other detector shapes than a line. In this paper we use a fiber-based annular detector for tomography. Thereby the sample is rotated inside the annular detector on a position different from the symmetry axis of the annular detector. Hence the sample is enclosed by the detector and all data from one plane are collected at once. By moving the detector parallel to the symmetrie axis of the ring one can acquire data for a 3D image reconstruction. Therfore, tomography can be performed with only one rotation axis and one translation axis. For image reconstruction a novel algorithm is necessary which was tested on simulated data. Here we present an imaging setup using such a fiber-based annular detector. First measurements of simple structures and subsequent image reconstruction from these real data are shown in this paper.

Keywords: annular detector, fiber-based detector, photoacoustic imaging

1. INTRODUCTION

Photoacoustic imaging (PAI) is an upcoming imaging technology in the field of medical and biological imaging.[1] In PAI a short pulse of electro-magnetic radiation (e.g. a short laser pulse) excites broadband ultrasonic waves (photoacoustic signal) due to thermoelastic expansion after absorption of the energy. Hence in photoacoustic imaging optical absorption of electromagnetic energy can be reconstructed at ultrasonic resolution, thus combining the advantages of optical imaging (high contrast) and ultrasonic imaging (high spatial resolution). For detection of photoacoustic signals usually conventional point like piezo-electric detectors are used, but also more unique detection schemes exist, e.g. interferometric foils[2,3] or, so called, integrating detectors. The latter were introduced in 2004 by Haltmeier et al.[4]

Since 2004 several approaches of integrating area detectors[5] and integrating line detectors[6–10] detectors were realized and showed their applicability for tomographic imaging. Beside the implementation of piezo-electric line detectors and free-beam interferometers acting as line detector several types of fiber-based line detectors were investigated by our group.[11–13] There are several advantages of using fiber-based detectors. Interferometric free-beam line detectors are focused to a small detection diameter. While near the beam waist good spatial resolution can be achieved, the resolution gets worse further away from the waist. Therefore a focused free-beam line detector is predestinated for high-resolution μ-tomography.[9] For bigger samples a fiber-based line detector is preferable due to the constant detection diameter along the detector. This results in uniform high resolution

Further author information: hubert.gruen@recendt.at

for big samples. Another advantage, compared to piezo-electric detectors, is the transparency of fiber (or free-beam) detectors. For excitation of photoacoustic signal the sample should be illuminated homogeneous from all sides. Using fiber-based detectors allows such a homogeneous illumination. Another advantage is the flexibility of fiber-based detectors. Thus, one has the possibility create new detector shapes.

Bending an integrating fiber-based line detector into an annular shape discloses new possibilities of integrating detectors. For example, annular detectors with a big diameter could be used for breast imaging. Thereby the diameter of the annular detector has to be much bigger than the human breast. Implementation in a small animal imager for pre-clinical studies is another possible application.

If one has already a working fiber-based detection setup realization of an annular detector is straightforward. Only the the fiber has to be brought to a annular shape, the rest of the setup keeps unmodified. Berer et al.[14] realized an annular detector with a relatively small diameter for photoacoustic microscopy. The annular detector, which was moved along a detection surface, collected focused signals originating from the symmetry axis of the ring. Zangerl et al.[15] proposed the use of an annular detectors with big diameter for tomography instead of microscopy and presented results using simulated data of spheres. For this tomographic approach the sample is placed on a position inside the annular detector. Thereby the axis of rotation of the sample has to be different from the axis of the annular detector. As the sample is enclosed by the detector all data from one plane are collected at once. Thus using an annular detector leads to a simple tomographic setup - only one rotation axis and one linear stage is needed.

In this work we present a brief summary of image reconstruction and the implementation of an annular detector for photoacoustic tomography. First results of real measurements on a wax ball and 2D image reconstruction will be presented. Afterward we discuss practical difficulties of realizing the annular detector and further improvements.

2. IMAGE RECONSTRUCTION USING ANNULAR DETECTORS

Positioning a small object inside an annular detector and measuring acoustic pressure for each position corresponds to a single measurement with an array of annular detectors as depicted in Fig. 1. For this setup it is beneficial to describe acoustic wave propagation in $\mathbb{R}^3$ in cylindrical coordinates

$$(z, r, \alpha) \mapsto (r\cos(\alpha), r\sin(\alpha), z),\ (z, r, \alpha) \in \mathbb{R} \times \mathbb{R}_{>0} \times [0, 2\pi]. \tag{1}$$

If $p(z, r, \alpha, t)$ denotes the acoustic pressure in cylindrical coordinates (1) at time t the annular detector at height z measures the signal that is proportional to the integral

$$G(z, t) = \frac{1}{2\pi} \int_0^{2\pi} p(z, r_{\text{det}}, \alpha) d\alpha\,, \tag{2}$$

where r_{det} denotes the radius of a circular detector. From these data a circular projection of the initial wave field f (representing the imaged object) can be reconstructed. More precisely this means that we can reconstruct

$$F(z, r) = \frac{1}{2\pi} \int_0^{2\pi} f(z, r, \alpha) d\alpha, \tag{3}$$

from G. In reference[15] series type reconstruction formulas that relate the projection F and the data G by means of integral transforms have been derived. Such a formula is for instance given by the expression

$$F(z, r) = \frac{2}{\pi^2 r_{\text{det}}^2} \int_{\mathbb{R}} \left(\sum_{n \in \mathbb{N}} \frac{\mathbf{F}_t \left\{ \mathbf{F}_z \left\{ G_\sigma^C \right\} \right\} (k, \sqrt{k^2 + v_n^2})}{H_0^{(2)}(r_{\text{det}} v_n) \sqrt{k^2 + v_n^2}} \frac{J_0(r v_n)}{J_1(r_{\text{det}} v_n)^2} \right) e^{ikz} dk\,, \tag{4}$$

where $H_0^{(2)}$ denotes the Hankel function of 0–th order of the the second kind. Furthermore J_0 and J_1 denote the Bessel functions of order 0 and 1, the v_n are the roots of the function $v \mapsto J_0(r_{\text{det}} v)$ and $\mathbf{F}$ denotes the Fourier transform where the index indicates the variable to which it is applied.

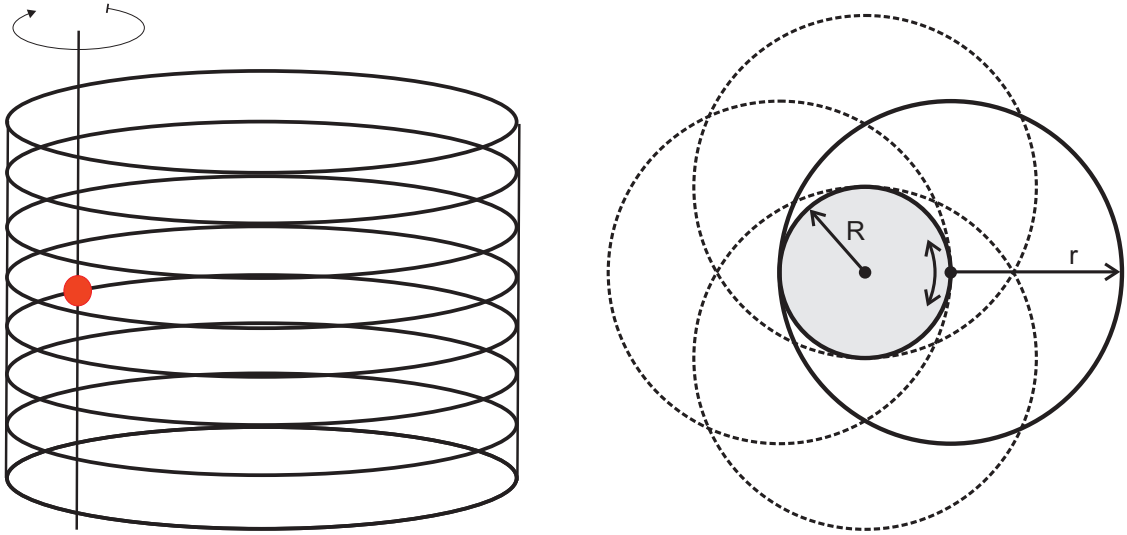

Figure 1. Left: A small object is placed inside an array (stack) of circular detectors and is rotated. Right: The cross section of the setup (where the circles are rotated instead of the object). The auxiliary quantity F reconstructed by Eq.4 provides all circular integrals of $f|_{\mathbb{R}^2\times\{z_0\}}$ over the circles centered on the circle of radius R. Note that R is the distance of the object to the axis of the cylindrical stack.

Rotating the object inside the stack of annular detectors by an angle σ yields several projections of the object f which is denoted by $F_\sigma(z,r)$. Fixing the variable $z = z_0$, see Fig. 1, yields the integral of $f|_{\mathbb{R}^2\times\{z_0\}}$ over concentric circles that are centered on a circle again. Inversion formulas for $f|_{\mathbb{R}^2\times\{z_0\}}$ from this particular family of integrals have been developed recently in.[16,17] Applying one of these formulas for each z gives a 3D reconstruction of the object f.

3. FIBER-BASED ANNULAR DETECTOR SETUP

As detector an fiber-based Mach-Zehnder interferometer using a perfluorinated graded index polymer optical fiber (perfluorinated GIPOF) as described by Grün et al.[18] was used. The setup consists of single mode glass fibers, but the sensitive part of the setup is build with the more sensitive GIPOF (compared to glass fibers). A scheme of the setup can be seen in Fig. 2. Instead of the previously used straight-line geometry of the detector the fiber was bent to an annular shape. As an exact circular geometry of the fiber is essential, the fiber is fixed on a fiber holder. The fiber holder consists of a thin board of acrylic glass with a circular hole. The fiber is glue into a notch on the inner surface of the hole, ensuring a perfect annular shape. A photograph of the fiber holder is depicted in Fig. 3. Back reflection from the end face of the holder which may occur is minimized by a zigzag pattern at the circumference. This zigzag pattern scatters the reflected waves. This pattern can also be seen in Fig. 3.

For photoacoustic tomography with integrating line detectors a horizontal illumination was used due to the transparency of the fiber-based detectors. Because of the shadowing effects of the detector holder this horizontal illumination is not possible for measurements using the annular detector. Therefore, the sample was illuminated in an certain angle from the upper side and the lower side as depicted in Fig. 4. This way illumination without shadowing was guaranteed independent of the height position of the annular detector.

4. MEASUREMENTS AND RECONSTRUCTION

First measurements were done using a ball made of black wax with a diameter of 3.5mm as sample. The object was placed in the annular detector with an radius of 20 mm at a position 13.6 mm away from the axis of the annular detector. Data were acquired at 200 different angles (increment of 1.8 degrees) at each height position z. These measurements were repeated on 80 different height positions covering a total 40 mm with an increment

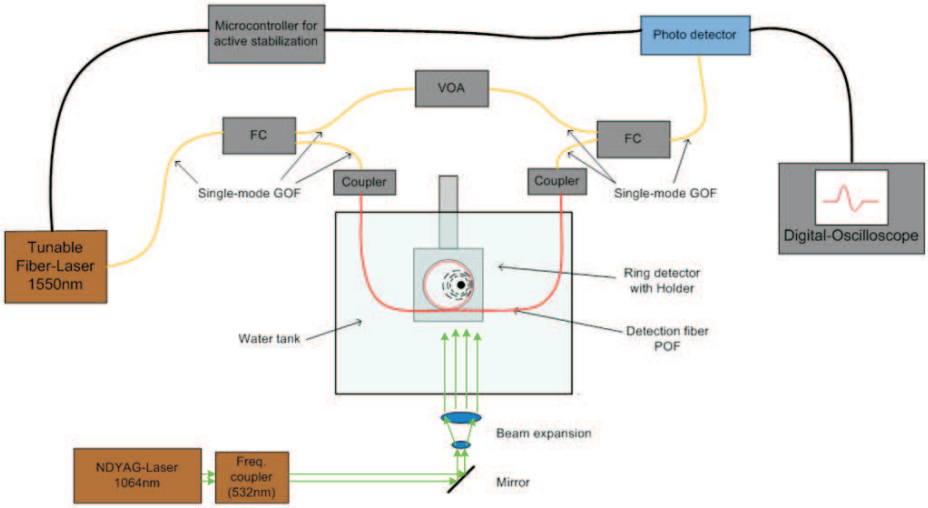

Figure 2. Schematic of the used fiber-based annular detector. The Mach-Zehnder detector was build up mainly with single mode glass optical fibers (GOF). Only for the detection path of the interferometer a more sensitive perfluorinated polymer optical fiber (POF) was used. The object is placed on a position different from the rotation axis of the annular detector.

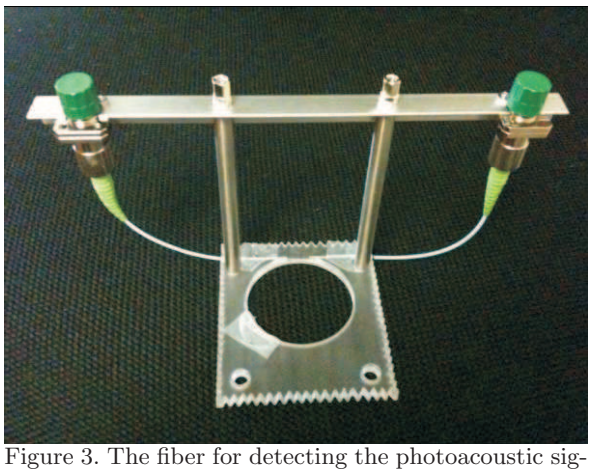

Figure 3. The fiber for detecting the photoacoustic signals is glued into a circular notch in a slice of acrylic glass. To prevent the contact of water with the connectors these are installed on top of the detector holder. The pattern on the circumference of the acrylic board decreases back reflections of waves which are coupled into the slice of acrylic glass.

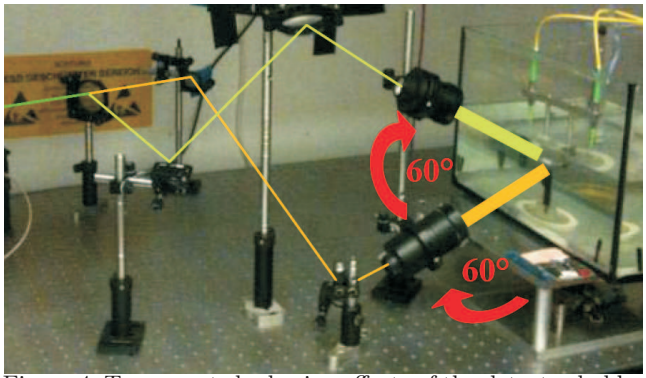

Figure 4. To prevent shadowing effects of the detector holder the illumination is not horizontal but under certain angles.

of 0.5 mm. The wax ball was placed in the middle of the hight positions at a high of 20mm. Every signal was recorded for a time period of $40\mu s$ (10000 data points) and was averaged 64 times.

For excitation of photoacoustic signals laser pulses with a duration of 10 ns, a repetition rate of 20 Hz, a wavelength of 532 nm and a pulse energy of 100 mJ were used. The laser beam was divided into two beams and expanded to a diameter of 18 mm as can be seen in Fig. 4. Therefore, we could maintain excitation values below the limits for tissue ($20\mathrm{mJ/cm^2}$).

Measured pressure curves for different heights at a fixed angle are plotted in Fig. 5. For image reconstruction the data were linearly interpolated between the 80 height positions to get more data points and superior image quality. For comparison simulated data are depicted in Fig. 6. While both pictures look largely similar two main differences can be seen. First, two additional signals appear in the measured signal. Comparison with the simulated data identifies the two correct curves at the abscissa positions of about 200 and 1000. Second, the curves are not as "smooth" as the simulated data. The latter difference can be easily explained. While the data were simulated presuming a solid sphere the measured signals originate only from a spherical shell. This is because the excitation wavelength is absorbed only in the outer layer of the wax ball. More remarkable are the two additional signals which can be seen clearly in the measured data and which are not from the wax ball. One can be seen at a position of approx. 1350 at the abscissa. Dealing with this artifact is easy. It can be cut off due to the fact that it appears later than the last possible correct signal (estimating object - detector distance and speed of sound in the water). The origin of this signal is unclear. However, as it remains at the same position of the entire scan length, it could be associated to the generation laser pulse cycle, e.g. electrical noise from the flash lamps or anything comparable. Not so easy is the dealing with the second artifact - the curve at the abscissa position of approx. 600. This signal appears between the correct signals and has an amplitude of the same order than the correct signal. This results is some difficulties during image reconstruction. Up to now it is still unclear what the origin of this additional signal is. This could be for example a reflected signal caused by the impedance mismatch of water and the detector holder made of PMMA.

From the measured and simulated data reconstructions were made. The reconstruction from the simulated data is shown in Fig. 8). The sphere can be clearly identified. Reconstruction form the measured data was, however, not successful. Due to the additional pressure curves the reconstruction was disturbed and superimposed artifacts appeared. Therefore, the region between the presumed correct pressure curves, containing the two artifacts, was set to zero. From these data a reconstruction was made. A 2D projection image of the wax ball is shown in Fig. 7. The outer shell of the wax ball can clearly be identified. As the excitation laser energy at a wavelength of 532 nm is absorbed completely at the outer shell no internal structures can be imaged.

These first imaging results - using modified data - show the proof of principle of an annular detector for photoacoustic tomography. However, there are several needs for improvements. Most important, the problem with the additional signals in the measured data has to be solved. The origin of the additional pressure curves has to be identified. Then, the fiber holder has to be redesigned to avoid these artifacts. There may be need for geometrical corrections, or the use of a different better acoustically matched material of the fiber holder. Also the measuring routine should be modified: using smaller increments for the height position results in better spatial resolution of the reconstruction. Another important issue is limited data. Recording the pressure data at different height positions leads to a cylindrical detection surface. To record data for the complete solid angle would require an infinite scan range, which is of course not possible. Thus a limited scan range leads to limited data. To get sufficient data from an large angle the scan range should be increased, which leads to a large amount of data and to longer measuring times. This problem can be solved by non-equispaced height positions. While data near the source are scanned with small height increments, the scanning steps can be increased outside the source. This, however, needs an adaption of the reconstruction algorithm.

5. CONCLUSION AND OUTLOOK

The proof of principle using integrating ring detectors for photoacoustic tomography was shown. Imaging using an annular detector was performed using exposure below the medical limits for tissue. Also several possible applications for biomedical imaging using the proposed detector are discussed. However, several problem with the setup, e.g. the problem with the additional signals in the measured data, have to be solved. The detection

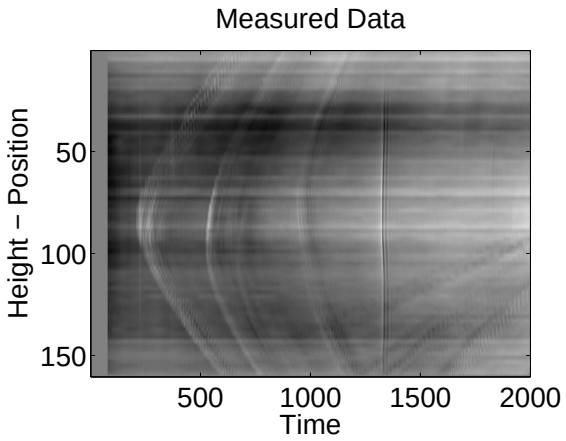

Figure 5. Measured data using the annular detector. The first and third pressure curve are signals from the wax ball. The second and last signals are two artifacts - but the last artifact is separably from the real data by time of flight.

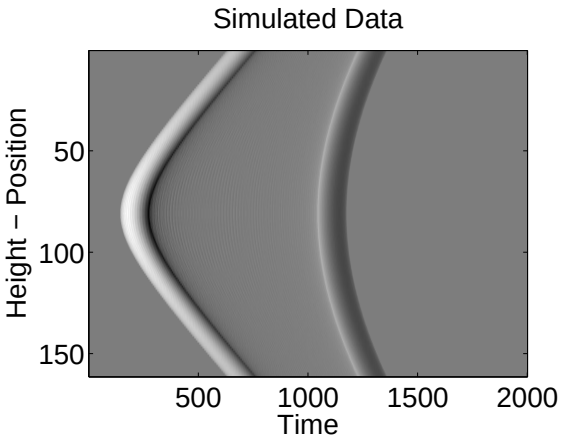

Figure 6. Simulated data for comparison - the pressure signals of the wax ball were simulated to identify where we should see a signal and which signals are real and which signals are artifacts. For the simulation all parameters were adapted to the real measurement.

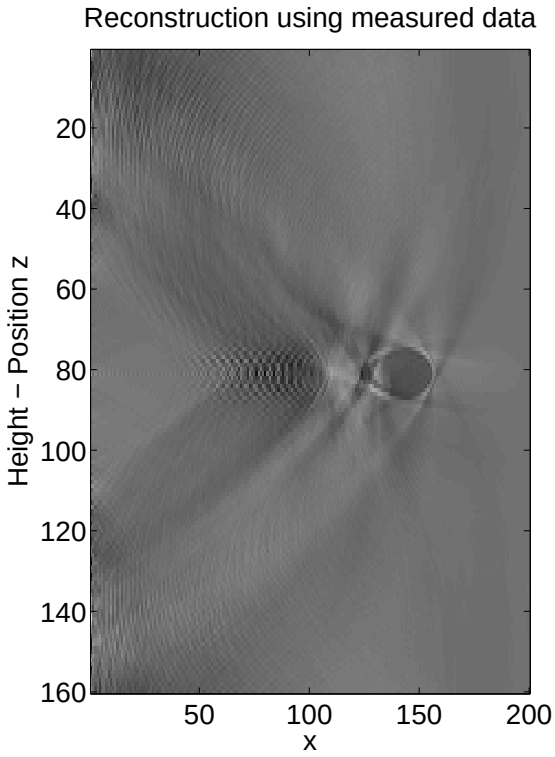

Figure 7. Reconstructed wax ball from measured and modified data. The shape, location and dimension can be reproduced correct Due to the superficial absorption at a wavelength of 532nm only the surface of the wax ball can be reconstructed.

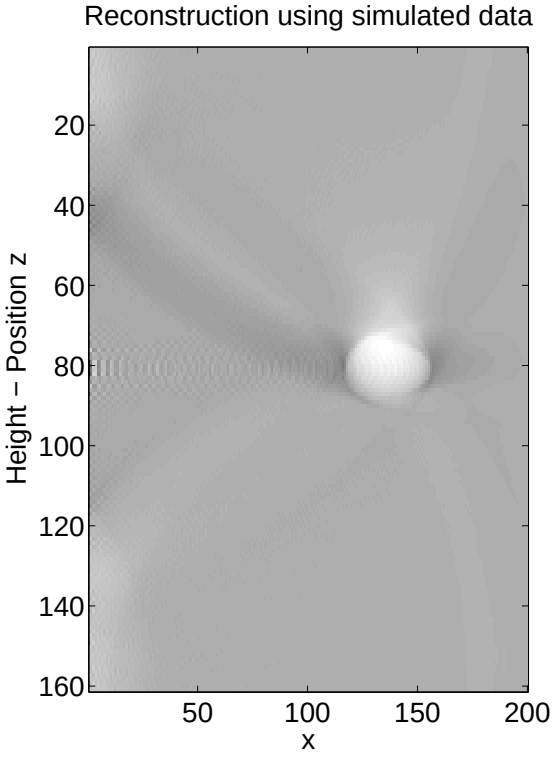

Figure 8. Reconstruction of the ball using the simulated data (see Fig. 6) for comparison with the measured data in Fig. 7. For simulation all parameters were matched to the real measurements for a fair comparison.

setup has to be analyzed and the detector holder has to be redesigned. Better scanning parameters, e.g. a non-equispaced height scan and covering a larger solid angle, will increase image quality and spatial resolution of the reconstructed images.

ACKNOWLEDGMENTS

This work has been supported by the Austrian Science Fund (FWF), project numbers S10502-N20, S10503-N20, S10505-N20 and TRP 102-N20, by the European Regional Development Fund (EFRE), and the federal state Upper Austria.

REFERENCES

[1] Wang, L. V., "Prospects of photoacoustic tomography," *Medical Physics* **35**, 5758–5767 (2008).

[2] Zhang, E. Z., Laufer, J., Pedley, R., and Beard, P., "In vivo high-resolution 3d photoacoustic imaging of superficial vascular anatomy," *Phys. Med. Biol.* **54**, 1035–1046 (2009).

[3] Hou, Y., Huang, S., Ashkenazi, S., Witte, R., and O'Donnel, M., "Thin polymer etalon arrays for high-resolution photoacoustic imaging," *Journal of Biomedical Optics* **13** (2008).

[4] Haltmeier, M., Scherzer, O., Burgholzer, P., and Paltauf, G., "Thermoacoustic computed tomography with large planar receivers," *Inverse Problems* **20**, 1663–1673 (2004).

[5] Burgholzer, P., Hofer, C., Paltauf, G., Haltmeier, M., Scherzer, O., Reitinger, B., and Höglinger, O., "Thermoacoustic tomography with integrating area and line detectors," *IEEE Transactions on Ultrasonics, Ferroelectrics and Frequency Control* **52**, 1577–1583 (2005).

[6] Paltauf, G., Nuster, R., and Burgholzer, P., "Characterization of integrating ultrasound detectors for photoacoustic tomography," *Journal of Applied Physics* **105** (2009).

[7] Paltauf, G., Nuster, R., Haltmeier, M., and Burgholzer, P., "Three-dimensional photoacoustic tomography using acousitc line detectors," in [*Biomedical Optics: Photons Plus Ultrasound: Imaging and Sensing 2007*], Oraevsky, A. A. and Wang, L. H., eds., *Proc. SPIE* **6437** (2007).

[8] Paltauf, G., Nuster, R., Haltmeier, M., and Burgholzer, P., "Photoacoustic tomography using a mach-zehnder interferometer as acoustic line detector," *Applied Optics* **46**, 3352–3358 (2007).

[9] Nuster, R., Holotta, M., Grossauer, H., Burgholzer, P., and Paltauf, G., "Photoacoustic micro-tomography using interferometric detection," *Journal of Biomedical Optics* **15** (2010).

[10] Nuster, R., Paltauf, G., Ditlbacher, H., and Burgholzer, P., "Integrated waveguide sensor for acoustic wave detection in photoacoustic tomography," in [*Biomedical Optics: Photons Plus Ultrasound: Imaging and Sensing 2008*], Oraevsky, A. A. and Wang, L. H., eds., *Proc. SPIE* **6856** (2008).

[11] Grün, H., Berer, T., Nuster, R., Paltauf, G., and Burgholzer, P., "Three dimensional photoacoustic imaging using fiber-based line detectors," *Journal of Biomedical Optics* **15**, 021306–1 – 021306–8 (2010).

[12] Grün, H., Berer, T., Pühringer, K., Nuster, R., Paltauf, G., and Burgholzer, P., "Polymer fiber detectors for photoacoustic imaging," in [*Biomedical Optics: Photons Plus Ultrasound: Imaging and Sensing 2010*], Oraevsky, A. A. and Wang, L. H., eds., *Proc. SPIE* **7564**, 75640M (2010).

[13] Grün, H., Haltmeier, M., Paltauf, G., and Burgholzer, P., "Photoacoustic tomography using a fiber based fabry-perot interferometer as an integrating line detector and image reconstruction by model-based time reversal method," in [*European Conferences on Biomedical Optics: Novel Optical Instrumentation for Biomedical Applications III*], Depeursinge, C. D., ed., *Proc. SPIE* **6631** (2007).

[14] Berer, T., Grün, H., Hofer, C., and Burgholzer, P., "Photoacoustic microscopy with large integrating optical annular detectors," in [*European Conferences on Biomedical Optics: Novel Optical Instrumentation for Biomedical Applications IV*], Depeursinge, C. D., ed., *Proc. SPIE* **7371** (2009).

[15] Zangerl, G., Scherzer, O., and Haltmeier, M., "Exact series reconstruction in photoacoustic tomography with circular integrating detectors," *Communications in Mathematical Sciences* **7**(3), 665 – 678 (2009).

[16] Finch, D., Haltmeier, M., and Rakesh, "Inversion of spherical means and the wave equation in even dimensions," *SIAM J. Appl. Math.* **68**, 392–412 (2007).

[17] Kunyansky, L., "Explicit inversion formulas for the spherical mean transform," *Inverse Problems* **23**, 373–383 (2007).

[18] Grün, H., Berer, T., Nuster, R., Paltauf, G., and Burgholzer, P., "Fiber-based detectors for photoacoustic imaging," in [*European Conferences on Biomedical Optics: Novel Optical Instrumentation for Biomedical Applications IV*], Depeursinge, C. D., ed., *Proc. SPIE* **7371** (2009).